INTERNATIONAL JOURNAL FOR NUMERICAL METHODS IN FLUIDS, VOL. 11, 177–188 (1990)

THE EFFECT OF USING NON-ORTHOGONAL BOUNDARY-FITTED GRIDS FOR SOLVING THE SHALLOW WATER EQUATIONS

PER NIELSEN AND OVE SKOVGAARD

Laboratory of Applied Mathematical Physics, Technical University of Denmark, Building 303, DK-2800 Lyngby, Denmark

SUMMARY

The purpose of this paper is to examine the effects of using non-orthogonal boundary-fitted grids for the numerical solution of the shallow water equations. Two geometries with well known analytical solutions are introduced in order to investigate the accuracy of the numerical solutions. The results verify that a reasonable departure from orthogonality can be allowed when the rate of change of cell areas is kept sufficiently small (i.e. it is not necessary to create a strictly orthogonal grid when the grid is sufficiently smooth).

KEY WORDS Shallow water equations Boundary-fitted grids

1. INTRODUCTION

The development in computer technology has given rise to extraordinary progress in the area of computational fluid dynamics (CFD). During the last decade computers have been made larger and faster, thus making it possible to model more complex flow domains. One of the most important problems in CFD today is the creation of a suitable grid needed in the numerical algorithms (i.e. finite difference, finite volume, finite element).

Many efforts have been made to develop methods for the automatic generation of grids for arbitrary flow regions, and as a result several automatic grid generation algorithms now exist involving both structured and unstructured grids.[1-3] Conventional Cartesian grids have been used and are still used to solve CFD problems. A disadvantage to this approach, however, is that the physical boundaries are represented in a 'staircase fashion'. An alternative approach is to use unstructured grids, but such grids require much more computational effort. A new and very promising approach is to generate curvilinear structured grids that conform to the boundaries.[1-3]

Curvilinear grids are particularly used in the field of aerodynamics, i.e. for flow calculations around aircraft and space shuttles. In the field of hydraulics this numerical technique is still being developed, but it is believed that the use of such curvilinear grids will result in more accurate numerical solutions. The grids are in general non-orthogonal, because orthogonality puts many constraints on the grid. Besides, it is difficult to implement orthogonality in three dimensions. It can be shown under appropriate assumptions that reasonable deviations from orthogonality are of little concern when the rate of change of cell areas is not too large.[1] This derivation is based on Taylor series expansion and on the assumption that the grid cells consist of parallel lines. It is the

0271–2091/90/100177–12$06.00

Received June 1989
Revised October 1989

aim of this paper to verify this statement by solving a flow problem using skewed grids. For this purpose the so-called shallow water equations are introduced. These equations describe the flow of an incompressible fluid subjected to gravity. In this paper the equations are solved for two geometries where analytical solutions exist. The analytical solutions are used to evaluate the accuracy of the numerical solutions.

The paper is organized as follows. First the grid generation scheme is described briefly. In order to be able to use curvilinear grids it is necessary to transform the flow equations to curvilinear co-ordinates. The discretization and the numerical solution of the flow equations are then constructed in these curvilinear co-ordinates. These procedures are described in Sections 2–4. Finally, a comparison of numerical and analytical results is presented in Section 5.

2. GRID GENERATION

In this work one of the well established methods for generating boundary-fitted grids is adopted. This is based on the solution of an elliptic partial differential system (Reference 1, Chap. VI). In two dimensions this is given by

$$\begin{aligned} g_{22}(x_{\xi\xi}+Px_{\xi})+g_{11}(x_{\eta\eta}+Qx_{\eta})-2g_{12}x_{\xi\eta}=0,\\ g_{22}(y_{\xi\xi}+Py_{\xi})+g_{11}(y_{\eta\eta}+Qy_{\eta})-2g_{12}y_{\xi\eta}=0, \end{aligned} \tag{1}$$

where g_{11}, g_{12} and g_{22} are metric norms given by

$$\begin{aligned} g_{11}&=x_{\xi}^2+y_{\xi}^2,\\ g_{12}&=x_{\xi}x_{\eta}+y_{\xi}y_{\eta},\\ g_{22}&=x_{\eta}^2+y_{\eta}^2. \end{aligned} \tag{2}$$

From these equations the physical co-ordinates (x, y) of the grid points, are generated from the specified curvilinear co-ordinates (ξ, η). P and Q are control functions used to control the grid line spacings and orientations. In this work these functions are evaluated from the arc length distribution on the boundary and from the boundary curvature.[4] This evaluation ensures that the grid lines generally follow the boundary point distribution.

3. TRANSFORMATION OF THE SHALLOW WATER EQUATIONS TO CURVILINEAR CO-ORDINATES

The shallow water equations describe the flow of a homogeneous incompressible fluid subjected to gravity. Neglecting the Coriolis force and the convective terms, these equations are given by[5, 6]

$$\begin{aligned} \frac{\partial u}{\partial t}&=-g\frac{\partial h}{\partial x} && \text{(momentum)},\\ \frac{\partial v}{\partial t}&=-g\frac{\partial h}{\partial y} && \text{(momentum)},\\ \frac{\partial h}{\partial t}&=-\frac{\partial(uH)}{\partial x}-\frac{\partial(vH)}{\partial y} && \text{(continuity)}, \end{aligned} \tag{3}$$

where g denotes the acceleration due to gravity, u and v are the horizontal z-independent velocity components, h is the surface elevation from the equilibrium level and H is the still water depth (see Figure 1).

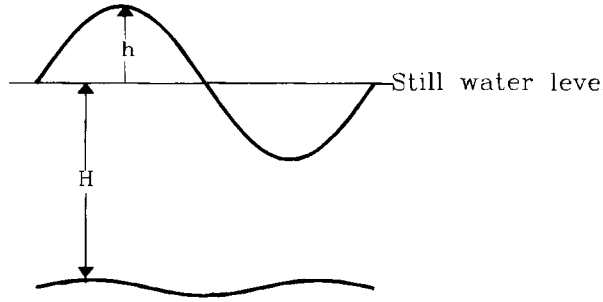

Figure 1. Geometry for the shallow water equations

In order to use the boundary-fitted grids, the flow equations have to be transformed to curvilinear co-ordinates. Details of this transformation can be found in References 7–9 and only the result will be quoted here:

$$\frac{\partial u}{\partial t}+\frac{g}{J}(h_\xi y_\eta - h_\eta y_\xi)=0 \qquad \text{(momentum)},$$

$$\frac{\partial v}{\partial t}+\frac{g}{J}(h_\eta x_\xi - h_\xi x_\eta)=0 \qquad \text{(momentum)}, \tag{4}$$

$$\frac{\partial h}{\partial t}+\frac{1}{J}[(uH)_\xi y_\eta-(vH)_\xi x_\eta+(vH)_\eta x_\xi-(uH)_\eta y_\xi]=0 \qquad \text{(continuity)}.$$

Here J denotes the Jacobian of the transformation given by

$$J=(g_{11}g_{22}-g_{12})^{1/2}. \tag{5}$$

It should be noted that the equations which describe the boundary conditions have to be transformed as well.

4. NUMERICAL PROCEDURE FOR THE SOLUTION OF THE SHALLOW WATER EQUATIONS

The transformed equations are approximated by finite difference approximations. Here an explicit method is used (central differences in the spatial co-ordinates and forward differences for the time derivatives). The solution is obtained by using a staggered grid with velocities defined at the full grids and the surface elevation at the half-grids. The discretization and the numerical solution procedure are detailed in References 7 and 8. The solution is obtained by using the following steps.

1. Specify the initial conditions to satisfy the analytical solution.
2. Advance the surface elevation in time by using the continuity equations.
3. Determine the velocities at the boundaries by using the boundary conditions.
4. Determine the velocities in the flow field by using the momentum equations.
5. Repeat steps 2–4 until the desired time.

5. TEST RESULTS

5.1. *Annular cylinders*

As a first example the shallow water equations are solved in the region between two concentric cylinders (see Figure 2). The vertical boundaries are here assumed to be solid walls. This requires that the normal velocity component vanishes. This boundary condition can be stated mathematically and transformed to curvilinear co-ordinates. Details of this derivation can be found in Reference 7; only the result will be quoted here:

$$\begin{aligned} &\frac{\partial u}{\partial t}+\frac{g\sin\varphi}{J}[\sin\varphi(h_\xi y_\eta - h_\eta y_\xi)-\cos\varphi(h_\eta x_\xi - h_\xi x_\eta)] = 0,\\ &\frac{\partial v}{\partial t}+\frac{g\cos\varphi}{J}[-\sin\varphi(h_\xi y_\eta - h_\eta y_\xi)+\cos\varphi(h_\eta x_\xi - h_\xi x_\eta)] = 0, \end{aligned} \tag{6}$$

where $(-\sin\varphi, \cos\varphi)$ denotes a unit tangent vector to the boundary. This is given by

$$\sin\varphi = -\frac{\dot{x}}{(\dot{x}^2+\dot{y}^2)^{1/2}}, \qquad \cos\varphi = \frac{\dot{y}}{(\dot{x}^2+\dot{y}^2)^{1/2}}, \tag{7}$$

where the dot denotes differentiation with respect to the boundary curve parameter (in this case one of the curvilinear co-ordinates).

The analytical solution can be found as a summation of different basic wave modes.[5,7] The modes are characterized by a mode number n that is equal to the number of waves in the azimuthal direction. With a proper choice of inner and outer radius, Neumann functions can be avoided.[7] This yields

$$J_n'(kr_1) = J_n'(kr_2) = 0, \tag{8}$$

where J_n denotes a Bessel function of the first kind of order n. In polar co-ordinates the wave modes are then given by

$$h(r, \theta, t) = h_0 J_n(kr)\cos(\omega t + n\theta), \tag{9}$$

where

$$\omega^2 = gH_0k^2 \tag{10}$$

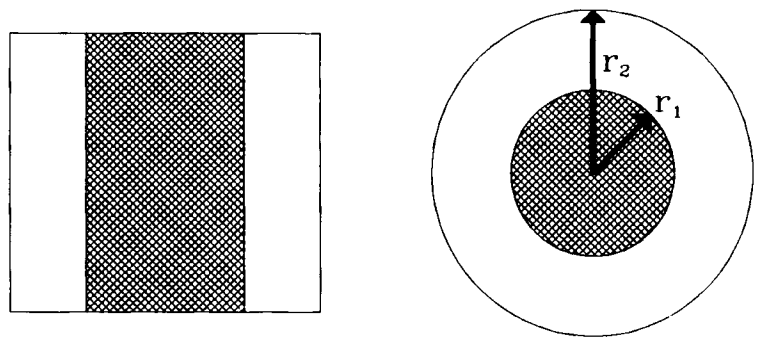

Figure 2. Annular cylinder geometry

and h_0 is a constant. In the present work k is chosen to be $k = 1$; r_1 and r_2 are then determined from (7).

The numerical results were obtained by using both orthogonal and skewed grids as well as uniform and non-uniform grids. All the calculations were done on grids with 119 grid lines in the radial direction and 25 grid lines in the azimuthal direction (in practice more grid lines would be needed in the azimuthal direction. The choice of 25 lines here is due to stability reasons for the explicit scheme on the non-uniform grids. In practice some kind of implicit scheme is preferable. The explicit scheme is only used here for the ease of coding.).

As a first result it was noted that the accuracy of the numerical solution was independent of the location of the grid points; i.e. the solution was as accurate at points near the boundaries as at points in the field. Furthermore, the accuracy of the solution was independent of the skewness when uniform grids were used (consistent with the result obtained in Reference 1 with appropriate assumptions).

Figures 3–5 show a comparison of the numerical solution with the analytical solution in the case $n = 2$ for

1. a skewed, uniform grid,
2. an orthogonal, non-uniform grid and
3. a skewed, non-uniform grid.

The skewed grids deviate far too much from orthogonality that would generally be allowed and rather serve as a worst case test, even though it is seen that accurate solutions are obtained on such grids. The larger phase error for the orthogonal, non-uniform grid compared to the skewed, uniform grid was found to be due to larger cell areas in the neighbourhood of that point where the solutions are shown. The amplitude error oscillates on the former grid, probably because of reduced smoothness. Finally, it is seen that the amplitude of the numerical solution on the skewed, non-uniform grid decreases with time. This amplitude decrease occurs at approximately the same rate in small and large cells.

It should be noted that one gets qualitatively the same results for other choices of n. The only difference is that the solution errors increase with n (as noted in Reference 7 for the case of orthogonal uniform grids). Furthermore, the results presented above are only for sufficiently smooth grids (the rate of change of cell areas is not too large). Preliminary results suggest that a lack in smoothness is more serious than a reasonable deviation from orthogonality.

5.2. *Paraboloid*

The numerical solution of the shallow water equations using boundary-fitted grids have been obtained in a rotating parabolic container in the special case where the water surface is always plane.[9] In this paper the equations are solved in a non-rotating parabolic container where the surface is not necessarily a plane. The depth profile in polar co-ordinates is given by (see Figure 6)

$$H = H_0\left[1 - \left[\frac{r}{a}\right]^2\right]. \tag{11}$$

The analytical solution to the problem is found in Reference 5 and is given as a double summation of wave modes characterized by the mode numbers n and s (s can be interpreted as the number of waves in the azimuthal direction). With specified values of n and s the solution is given by

$$h(r, \theta, t) = \sum_{m=s}^{n-2} A_m \left[\frac{r}{a}\right]^m \cos(s\theta) \cos \omega t, \quad m = s, s+2, \ldots, n-2, \tag{12}$$

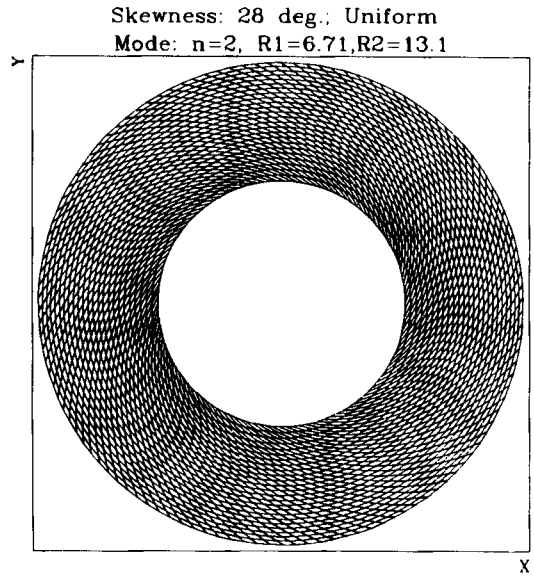

(a)

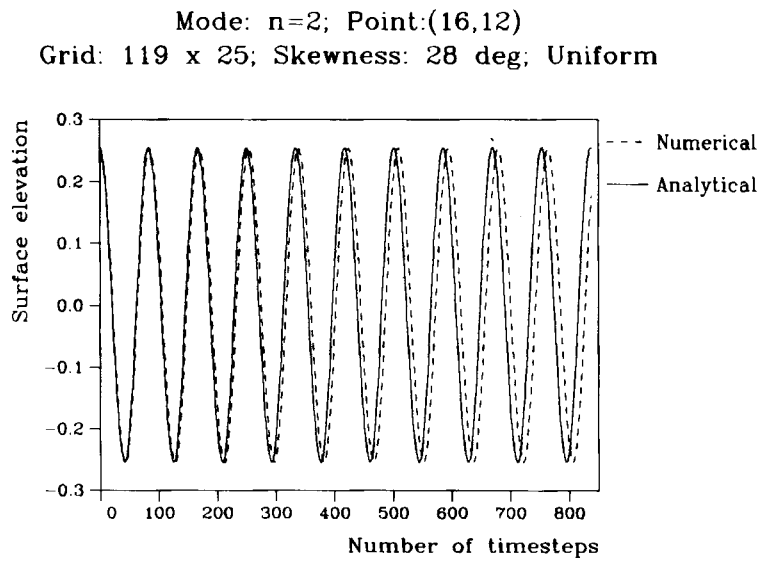

(b)

Figure 3. (a) Uniform grid with a skewness of approximately 28°. (b) Comparison of numerical and analytical solution for the annular cylinder

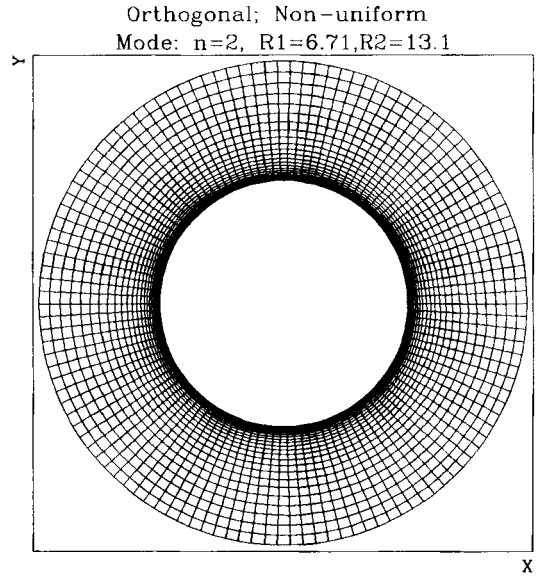

(a)

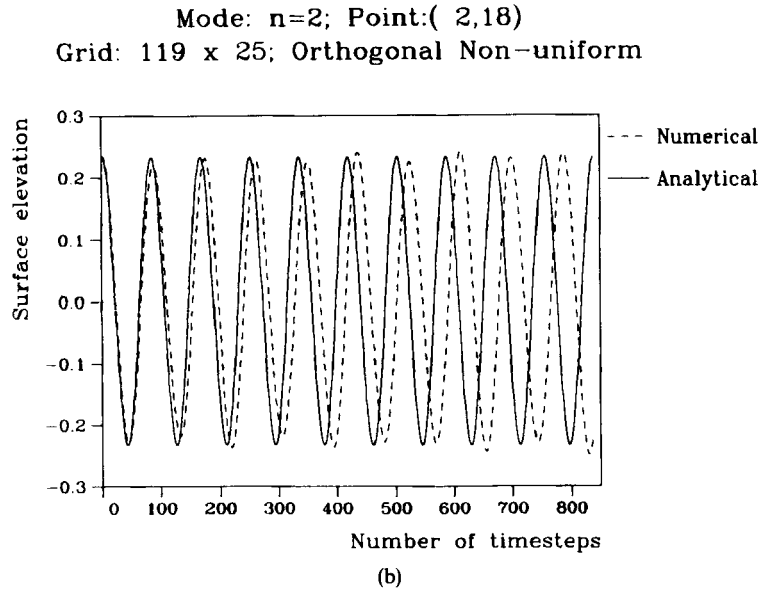

(b)

Figure 4. (a) Orthogonal non-uniform grid. (b) Comparison of numerical and analytical solution for the annular cylinder

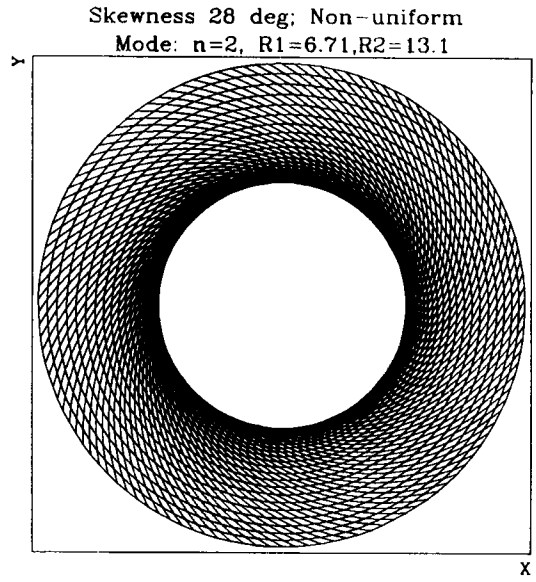

(a)

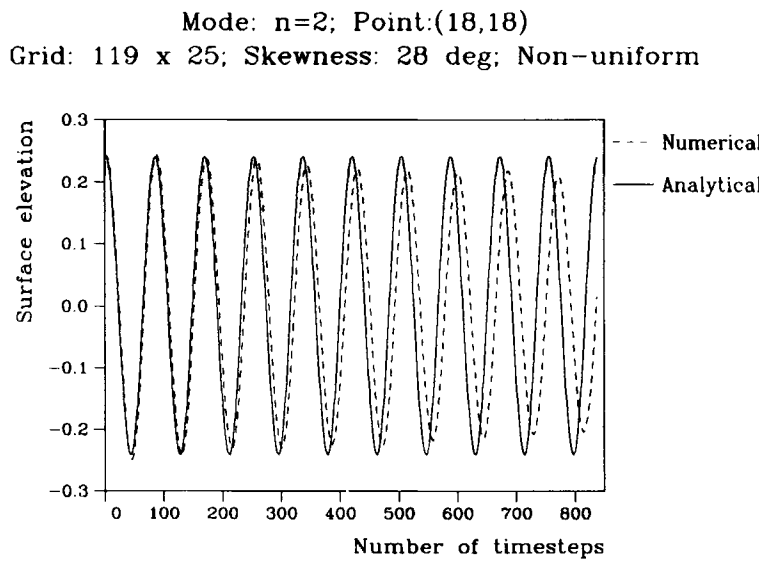

(b)

Figure 5. (a) Non-uniform grid with a skewness of approximately 28°. (b) Comparison of numerical and analytical solution for the annular cylinder

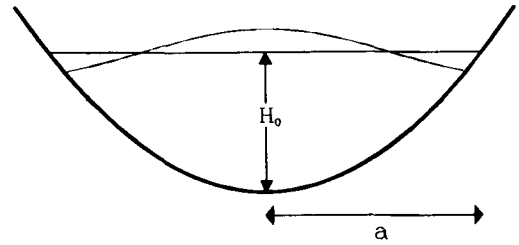

Figure 6. Paraboloid geometry

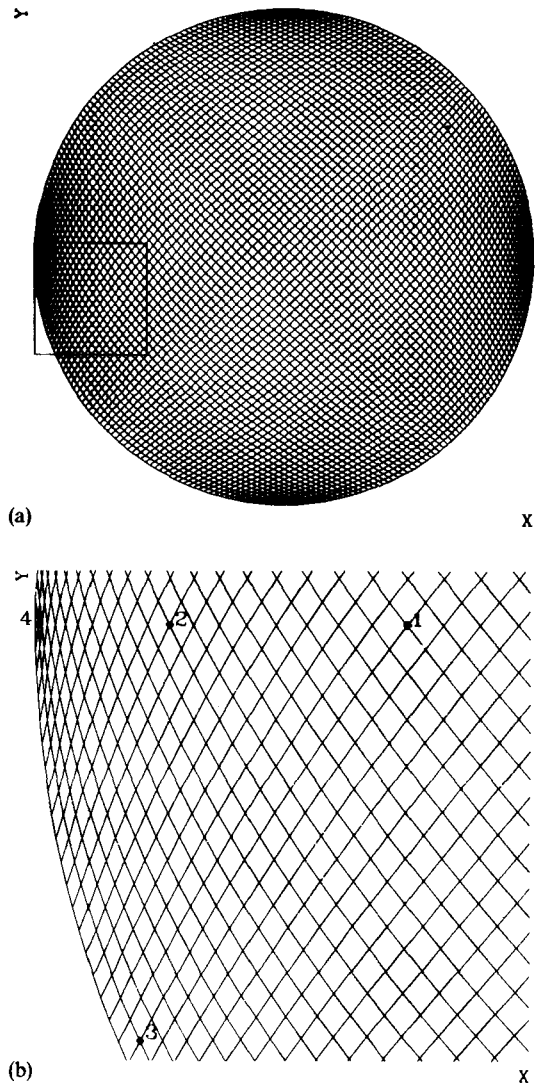

Figure 7. (a) Entire grid used in the parabolic test example. (b) Blow-up of a local region. Figures 8–11 show results at the points marked 1–4

where

$$\omega^2 = \frac{gH_0}{a^2}[n(n-2)-s^2] \tag{13}$$

and the coefficients A_m obey the recurrence relation

$$A_m = \frac{(m-n)(m+n-2)}{m^2-s^2}A_{m-2}, \quad m = s, s+2, \ldots, n-2. \tag{14}$$

The boundary condition involved in the analytical solution is that the surface elevation is finite at the boundary ($r = a$). Numerically this is simply implemented by requiring that the momentum equations should be satisfied.

The numerical solutions were generated by using a 73×73 grid as shown in Figure 7. The results showed that the numerical errors (both amplitude and phase) generally increased with the difference of the wave mode numbers $(n-s)$ (i.e. with the complexity of the flow pattern). Figures 8–11 show typical results in the case $s = 2, n = 6$ (one of the more complex flow patterns). It is seen that a larger departure from orthogonality does not generate considerable errors (not even on the boundary) except near singular points (see Figure 11) where there is a shift in co-ordinate family on the boundary. In general the phase errors tend to increase with time while the amplitude errors oscillate. The oscillations are most clearly seen at points near the boundaries. Furthermore, the amplitude errors seem to be of larger concern than the phase errors.

6. CONCLUSIONS

In this paper the effects of using non-orthogonal boundary-fitted grids have been examined. For this purpose the shallow water equations have been solved for two geometries with well known analytical solutions. The numerical solutions have been compared with the analytical solutions

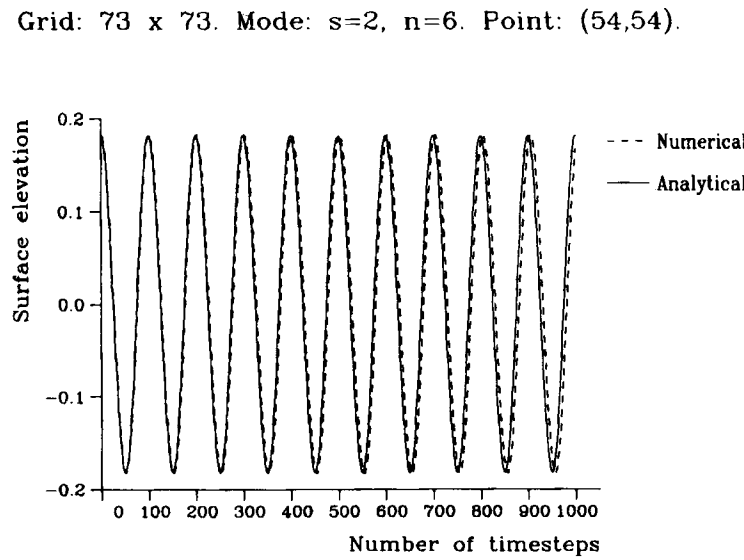

Figure 8. Comparison of numerical and analytical solution for the parabolic geometry at an interior point with local skewness of approximately 74° (point 1)

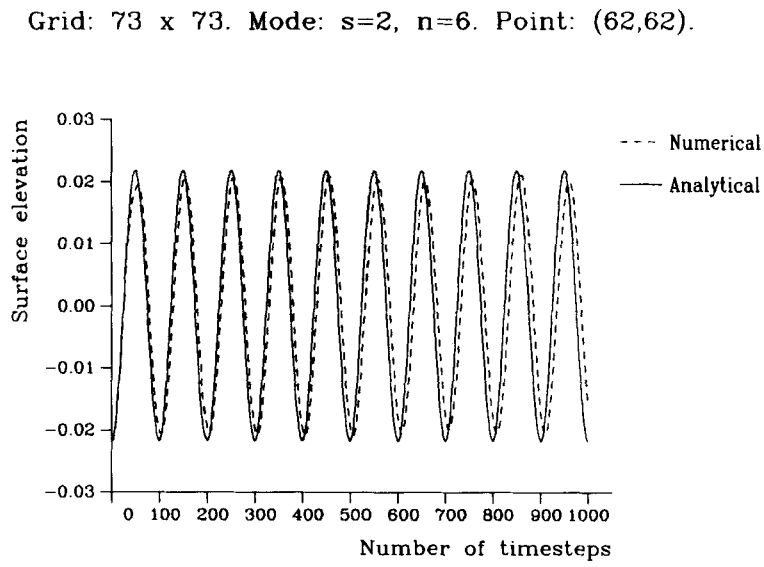

Figure 9. Comparison of numerical and analytical solution for the parabolic geometry at an interior point with local skewness of approximately 52° (point 2)

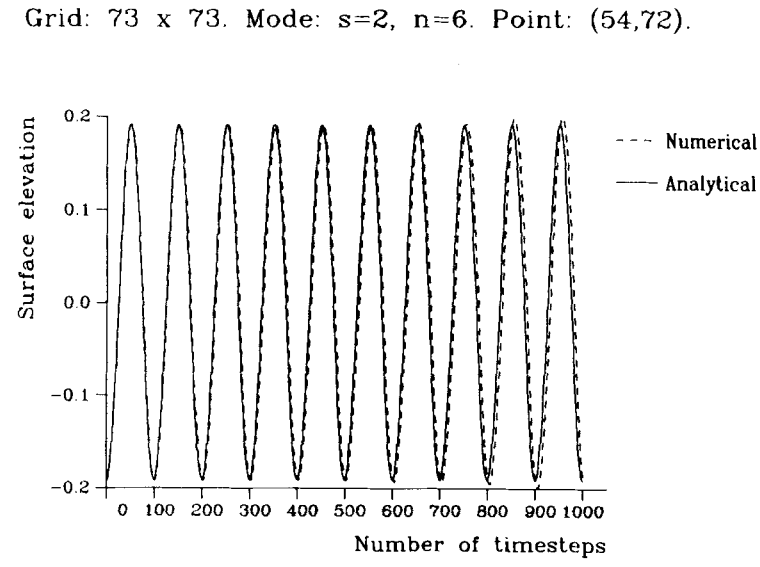

Figure 10. Comparison of numerical and analytical solution for the parabolic geometry at a point near the boundary with local skewness of approximately 52° (point 3)

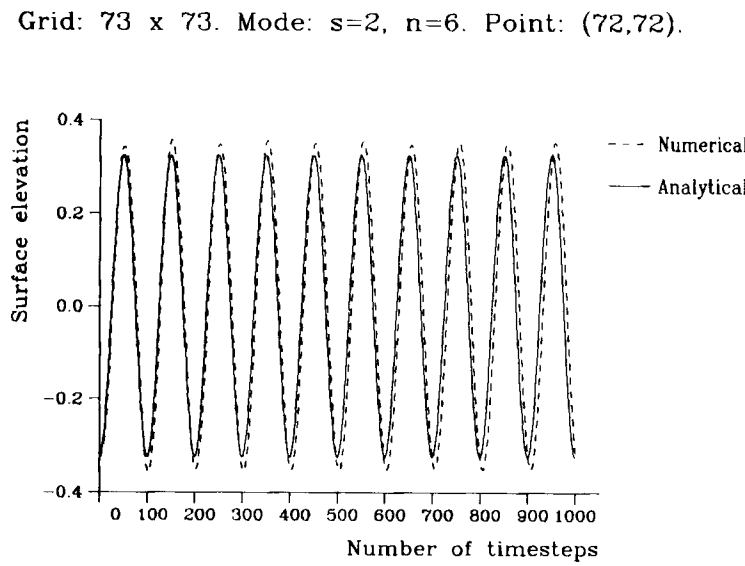

Figure 11. Comparison of numerical and analytical solution for the parabolic geometry at a point near a special point (point 4)

and the results show that reasonable departures from orthogonality only have small effects on the numerical accuracy when the grids are sufficiently smooth. However, it is more difficult to obtain accurate solutions near singular points on the boundaries. The numerical results verify the conclusion of the derivation given in Reference 1 with appropriate assumptions.

The use of Cartesian grids will generally result in larger errors than the use of boundary-fitted grids (see Reference 8). This is also true for skewed grids when the deviation from orthogonality is reasonable. From an engineering point of view it is therefore recommended to use boundary-fitted grids that are as smooth as possible without serious deviation from orthogonality.

ACKNOWLEDGEMENT

The financial support of the Danish Technical Research Council (through Contract No. 5.17.3.6.12 as a part of the FTU programme) is gratefully acknowledged.

REFERENCES

1. J. F. Thompson, Z. U. A. Warsi and C. W. Mastin, *Numerical Grid Generation—Foundations and Applications*, Elsevier, New York, 1985.
2. J. Hauser and C. Taylor (eds), *Numerical Grid Generation in Computational Fluid Dynamics*, Pineridge Press, Swansea, 1986.
3. S. Sengupta, J. Hauser, P. R. Eiseman and J. F. Thompson (eds), *Numerical Grid Generation in Computational Fluid Mechanics '88*, Pineridge Press, Swansea, 1988.
4. J. F. Thompson, 'A general three-dimensional elliptic grid generation system on a composite structure', *Comput. Methods Appl. Mech. Eng.*, **64**, 377–411 (1987).
5. H. Lamb, *Hydrodynamics*, 6th edn, Cambridge University Press, 1932.
6. M. B. Abbott, *Computational Hydraulics*, Pitman, London, 1979.
7. J. Hauser, H.-G. Paap, D. Eppel and A. Mueller, 'Solution of shallow water equations for complex flow domains via boundary-fitted co-ordinates', *Int. j. numer. methods fluids*, **5**, 727–744 (1985).
8. J. Hauser, H. G. Paap, D. Eppel and S. Sengupta, 'Boundary conformed co-ordinate systems for selected two-dimensional fluid flow problems. Part II: Application of the BFG method', *Int. j. numer. methods fluids*, **6**, 529–539 (1986).
9. R. Raghunath, S. Sengupta and J. Hauser, 'A study of the motion in rotating containers using a boundary fitted co-ordinate system', *Int. j. numer. methods fluids*, **7**, 453–464 (1987).